Appendix A24

Deterministic diffusion

A24.1 Diffusion in sawtooth and cat maps

(R. Artuso)

In this section we will deal with the prototype example of chaotic Hamiltonian maps, hyperbolic toral automorphisms. Diffusive properties will arise in considering such maps acting on the cylinder or over $\mathbb{R}^2$, while the dynamics restricted to the fundamental domain involves maps on $\mathbf{T}^2$ (two–dimensional torus). An Anosov map thus corresponds to the action of a matrix in $SL_2(\mathbb{N})$ with unit determinant and absolute value of the trace bigger than 2.

Maps of this kind are as examples of genuine Hamiltonian chaotic evolution. They admit simple finite Markov partitions, which paves the way to a good symbolic dynamics. Within the framework of Hamiltonian dynamical systems the role of hyperbolic linear automorphisms is analogous to piecewise linear Markov maps: their symbolic dynamics can be encoded in a grammatically simple way, and their linearity leads to uniformity of cycle stabilities.

chapter ??

We will consider the "two-coordinates" representation for them

$$\begin{bmatrix} x' \\ y' \end{bmatrix} = M \begin{bmatrix} x \\ y \end{bmatrix}$$

with

$$M = \begin{bmatrix} 0 & 1 \\ -1 & K+2 \end{bmatrix}$$

which allows considering their extension on a cylinder phase space ($[-1/2, 1/2) \times \mathbb{R}$) in a natural way. So it is natural to study diffusion properties along the y direction.

Though Markov partitions encode the symbolic dynamics in the simplest possible way, they are not well suited to deal with diffusion, as the jumping factor

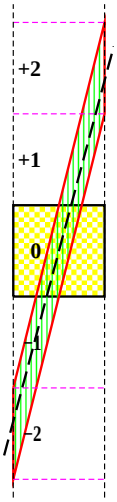

Figure A24.1: The elementary cell for the torus map $[-1/2, 1/2]$ (checkered yellow) together with its image, in green ($K = 2$): symbols refer to the linear code. The dashed line through the origin gives the direction of the unstable manifold. Though hardly understandable from the scale of the picture the unstable manifold is not parallel to the image sides.

is not related in a simple way to the induced symbol sequence. To this end the following linear code is quite natural: before describing it let us fix the notations: χ will denote the trace of the map ($\chi = K + 2$): the leading eigenvalue will be denoted by $\lambda = (\chi + \sqrt{D})/2$, where $D = \chi^2 - 4$. In principle the code (and the problem of diffusion) can be also considered for real values of K (thus loosing continuity of the torus map when K in not an integer): we will remark in what follows that results which are exact for $K \in \mathbb{N}$ are only approximate for generic K.

The cardinality of the alphabet is determined by the parameter K: the letters are integer numbers, whose absolute values does not exceed $Int(1 + \chi/2)$ (see figure A24.1 for the case $K = 2$). The code is linear, as, given a bi-infinite sequence $\{x_i\}_{i\in\mathbb{N}}$

$$b_t \stackrel{\text{def}}{=} \left[(K+2)x_t - x_{t-1} + \frac{1}{2}\right] \quad , \tag{A24.1}$$

$[\dots]$ denoting the integer part, while the inversion formula (once a bi-infinite symbolic string $\{b_i\}_{i\in\mathbb{N}}$ is given), reads

$$x_t = \frac{1}{\sqrt{D}} \sum_{s\in\mathbb{N}} \lambda^{-|t-s|} b_s \quad , \tag{A24.2}$$

As the x coordinate lives in the interval $[-1/2, 1/2)$, (A24.2) induces a condition of allowed symbol sequences: $\{b_i\}_{i\in\mathbb{N}}$ will be an admissible orbit if

$$\frac{1}{2} \le \frac{1}{\sqrt{D}} \sum_{s\in\mathbb{N}} \lambda^{-|t-s|} b_s < \frac{1}{2} \quad . \tag{A24.3}$$

By (A24.1)(A24.2) it is easy to observe that periodic orbits and allowed periodic symbol sequences are in one-to-one correspondence. From (A24.3) we get the condition that a $\{b_i\}_{i=1,\dots,T}$ sequence corresponds to a T–periodic orbit of the map

$$|A_n b_t + A_{n-1}(b_{t+1} + b_{t-1}) + \cdots + A_0(b_{t+n} + b_{t-n})| < \frac{B_n}{2} \quad \forall t = 1, \dots, T$$

when $T = 2n + 1$, and

$$|C_n b_t + C_{n-1}(b_{t+1} + b_{t-1}) + \cdots + C_0(b_{t+n})| < \frac{D_n}{2} \quad \forall t = 1, \ldots, T \qquad \text{(A24.4)}$$

when $T = 2n$ where

exercise A24.1
exercise A24.2

$$\begin{aligned} B_k &= \lambda^k(\lambda - 1) + \lambda^{-k}(\lambda^{-1} - 1) & A_k &= \frac{\lambda^{k+1} + \lambda^{-k}}{\lambda + 1} \\ D_k &= (\lambda^k - \lambda^{-k})(\lambda - \lambda^{-1}) & C_k &= \lambda^k + \lambda^{-k} \end{aligned} \qquad \text{(A24.5)}$$

The pruning rules (A24.4) admit a simple geometric interpretation: a lattice point $\boldsymbol{b} \in \mathbb{N}^T$ identifies a T–periodic point of the map if $\boldsymbol{b} \in \mathcal{P}_T$ where

$$\mathcal{P}_T \stackrel{\text{def}}{=} \{\boldsymbol{x} \in \mathbb{R}^T : \quad \left\{ \begin{array}{c} |a_1 x_1 + \cdots + a_T x_T| < e_T \\ \vdots \\ |a_2 x_1 + \cdots + a_1 x_T| < e_T \end{array} \right\} \qquad \text{(A24.6)}$$

and

$$\begin{aligned} a_1 \ldots a_T &= A_0 A_1 \ldots A_{n-1} A_n A_{n-1} \ldots A_0 & e_T &= B_n/2 \\ a_1 \ldots a_T &= C_1 \ldots C_{n-1} C_n C_{n-1} \ldots C_1 C_0 & e_T &= D_n/2 \end{aligned} \qquad \text{(A24.7)}$$

for $T = 2n+1$ or $T = 2n$, respectively, Thus $\mathcal{P}_T$ is a measure polytope [7], obtained by deforming a T–cube. This is the key issue of this appendix: though the map is endorsed with a most remarkable symbolic dynamics, the same is hardly fit to deal with transport properties, as the rectangles that define the partition are not directly connected to translations once the map is unfolded to the cylinder. The partition connected to the linear code (see figure A24.1) on the other side is most natural when dealing with transport, though its not being directly related to invariant manifolds leads to a multitude of pruning rules (which in the present example bear a remarkable geometric interpretation, which is not to be expected as a generic feature).

exercise A24.3

We will denote by $\mathcal{N}_{n,s}$ the number of periodic points of period n with jumping number s. By taking (**??**) into account we can easily see that for cat maps a way to compute D is provided by

$$D = \lim_{n\to\infty} D_n \qquad D_n = \frac{1}{n\mathcal{N}_n} \sum_{k=1}^{p(n)} k^2 \mathcal{N}_{n,k} \qquad \text{(A24.8)}$$

where $\mathcal{N}_n$ is the number of periodic points of period n, $p(n)$ is the highest jumping number of n–periodic orbits and we employed

$$\left|\det\left(\mathbf{1} - \boldsymbol{J}_x^{(n)}\right)\right| = (\lambda^n - 1)(1 - \lambda^{-n}) = \mathcal{N}_n$$

which is valid for cat maps.

Sums can be converted into integrals by using Poisson summation formula: we define

$$f_T(n) = \begin{cases} (n_1 + \cdots + n_T)^2 & n \in \mathcal{P}_T \bigcap \mathbb{N}^T \\ 0 & otherwise \end{cases}$$

and

$$\tilde{f}_T(\xi) = \int_{\mathbb{R}^T} dx\, e^{i(x,\xi)}\, f_T(x)$$

From Poisson summation formula we have that

$$D_T = \frac{1}{T\mathcal{N}_T} \sum_{n\in\mathbb{N}^T} \tilde{f}_T(2\pi n) \tag{A24.9}$$

The quasilinear estimate for D_T amounts to considering the $n = 0$ contribution to (A24.9):

$$D_T^{(q.l.)} = \int_{\mathcal{P}_T} dx\, (x_1 + x_2 + \cdots + x_T)^2 \tag{A24.10}$$

The evaluation of (A24.10) requires introducing a coordinate transformation in symbolic space in which $\mathcal{P}_T$ is transformed in a T–cube. This is equivalent to finding the inverse of the matrix A:

$$A \stackrel{\text{def}}{=} \begin{pmatrix} a_1 & a_2 & \cdots & a_{T-1} & a_T \\ a_T & a_1 & \cdots & a_{T-2} & a_{T-1} \\ \vdots & \vdots & \ddots & \vdots & \vdots \\ a_3 & a_4 & \cdots & a_1 & a_2 \\ a_2 & a_3 & \cdots & a_T & a_1 \end{pmatrix} . \tag{A24.11}$$

First of all let us observe that A is a circulant matrix, so that its determinant is the product of T factors, each of the form $f(\epsilon_j) = a_1 + \epsilon_j a_2 + \cdots + a_T \epsilon_j^{T-1}$, where ϵ_j is a Tth root of unity. By using (A24.5) it is possible to see that

$$f(\epsilon_j) = \begin{cases} \frac{\epsilon_j^{n+1} B_n}{(\lambda\epsilon_j - 1)(1 - \lambda^{-1}\epsilon_j)} & T = 2n+1 \\ \frac{\epsilon_j^{n} D_n}{(\lambda\epsilon_j - 1)(1 - \lambda^{-1}\epsilon_j)} & T = 2n \end{cases}$$

so that

$$|\det A| = \frac{(2e_T)^T}{\lambda^T + \lambda^{-T} - 2} \tag{A24.12}$$

By using the results coming from the former exercise we can finally express A^{-1} via exercise A24.4

$$\tilde{C}A^{-1} = \frac{1}{B_n^T} \begin{pmatrix} \chi & -1 & \cdots & 0 & -1 \\ -1 & \chi & \cdots & 0 & 0 \\ \vdots & \vdots & \ddots & \vdots & \vdots \\ 0 & 0 & \cdots & \chi & -1 \\ -1 & 0 & \cdots & -1 & \chi \end{pmatrix} \tag{A24.13}$$

where

$$\tilde{C} = \begin{pmatrix} \mathbf{0} & \mathbb{1}_{n+1} \\ \mathbb{1}_n & \mathbf{0} \end{pmatrix} \quad .$$

if $T = 2n + 1$ and

$$\tilde{K}A^{-1} = \frac{1}{D_n^T} \begin{pmatrix} \chi & -1 & \cdots & 0 & -1 \\ -1 & \chi & \cdots & 0 & 0 \\ \vdots & \vdots & \ddots & \vdots & \vdots \\ 0 & 0 & \cdots & \chi & -1 \\ -1 & 0 & \cdots & -1 & \chi \end{pmatrix} \tag{A24.14}$$

where

$$\tilde{K} = \begin{pmatrix} \mathbf{0} & \mathbb{1}_n \\ \mathbb{1}_n & \mathbf{0} \end{pmatrix} \quad .$$

if $T = 2n$. As a first check of quasilinear estimates let's compute the volume of $\mathcal{P}_T$:

$$\begin{aligned} Vol(\mathcal{P}_T) &= \int_{\mathcal{P}_T} dx_1\, dx_2 \ldots dx_T = \frac{1}{|\det A|} \int_{-e_T}^{e_T} \cdots \int_{e_T}^{e_T} d\xi_1 \ldots d\xi_T \\ &= \lambda^T + \lambda^{-T} - 2 \end{aligned} \tag{A24.15}$$

In an analogous way we may compute the quasilinear estimate for $\mathcal{N}_{T,k}$

exercise A24.5

$$\begin{aligned} \mathcal{N}_{T,k}^{(q.l.)} &= \int_{\mathcal{P}_T} dx_1 \ldots dx_T\, \delta(x_1 + \ldots x_T - k) \\ &= \frac{\lambda^T + \lambda^{-T} - 2}{(2e_T)^T} \int_{-\infty}^{\infty} d\alpha\, e^{-2\pi i \alpha k} \int_{-e_T}^{e_T} \cdots \int_{-e_T}^{e_T} d\xi_1 \ldots d\xi_T\, e^{\frac{2\pi i \alpha \chi}{2e_T}(\xi_1 + \cdots + \xi_T)} \\ &= \frac{2}{\pi\chi}(\lambda^T + \lambda^{-T} - 2) \int_0^{\infty} dy\, \cos\left(\frac{2qy}{\chi}\right)\left(\frac{\sin y}{y}\right)^T \end{aligned} \tag{A24.16}$$

where we have used $x_1 + \cdots + x_T = (\chi/(2e_T))(\xi_1 + \cdots + \xi_T)$ (cfr. (A24.13),(A24.14)).

We are now ready to evaluate the quasilinear estimate fo the diffusion coefficient

$$D_T^{(q.l.)} = \frac{1}{\pi\chi T} \int_{-T\chi/2}^{T\chi/2} dz\, z^2 \int_0^{\infty} dy\, \cos\left(\frac{2zy}{\chi}\right)\left(\frac{\sin y}{y}\right)^T \tag{A24.17}$$

(where the bounds on the jumping number again come easily from (A24.13),(A24.14)). By dropping terms vanishing as $T \mapsto \infty$, and using [10]

$$\int_0^{\infty} dx \left(\frac{\sin x}{x}\right)^n \frac{\sin(mx)}{x} = \frac{\pi}{2} \quad m \geq n$$

we can evaluate

$$D^{(q.l.)} = \frac{\chi^2}{24} \tag{A24.18}$$

which is the correct result [5] (and again for cat maps (A24.18) is not the quasilinear estimate but the exact value of the diffusione coefficient).

exercise A24.6

Commentary

Remark A24.1. Who has talked about it? Maps of this kind have been extensively analyzed as examples of genuine Hamiltonian chaotic evolution: in particular they admit simple Markov partitions [2, 9], which lead to simple analytic expressions for topological zeta functions [11]. The linear code was introduced by Percival and Vivaldi [4, 15]. Measure polytopes are discussed in ref. [7]. The quasilinear estimate (A24.10) was given in ref. [5]. (A24.10) was evaluated in ref. [3, 16]. Circulant matrix are discussed in ref. [1]. The result (A24.18) agrees with the saw-tooth result of ref. [5]; for the cat maps (A24.18) is the exact value of the diffusion coefficient. This result was obtained, by using periodic orbits also in ref. [8], where Gaussian nature of the diffusion process is explicitly assumed.

Remark A24.2. Phase space. The cylinder phase is $[-1/2, 1/2) \times \mathbb{R}$: the map is originally defined definition in $[-1/2, 1/2)^2$, and is generalized over the cylinder by symmetry requirements (24.21).

References

[1] A. C. Aitken, *Determinants and Matrices* (Oliver and Boyd, Edinburgh, 1956).

[2] V. I. Arnol'd and A. Avez, *Ergodic Problems of Classical Mechanics* (Addison-Wesley, Redwood City, 1989).

[3] R. Artuso and R. Strepparava, "Reycling diffusion in sawtooth and cat maps", Phys. Lett. A **236**, 469–475 (1997).

[4] N. Bird and F. Vivaldi, "Periodic orbits of the sawtooth maps", Physica D **30**, 164–176 (1988).

[5] J. R. Cary and J. D. Meiss, "Rigorously diffusive deterministic map", Phys. Rev. A **24**, 2664–2668 (1981).

[6] C.-C. Chen, C.-C. Chen, and N. C.-H. U. T. preprint, Diffusion coefficient of piecewise linear maps, 1994.

[7] H. S. M. Coxeter, *Regular Polytopes* (Dover, 1948).

[8] I. Dana, "Hamiltonian transport on unstable periodic orbits", Physica D **39**, 205 (1989).

[9] R. L. Devaney, *An Introduction to Chaotic Dynamical systems*, 2nd ed. (Westview Press, 2008).

[10] I. S. Gradshteyn and I. M. Ryzhik, *Tables of integrals, series and products* (Academic, New York, 1980).

[11] S. Isola, "ζ-functions and distribution of periodic orbits of toral automorphisms", Europhys. Lett. **11**, 517–522 (1990).

[12] R. Klages, *Deterministic Diffusion in One-dimensional Chaotic Dynamical Systems* (Wissenschaft and Technik-Verlag, Berlin, 1996).

[13] R. Klages and J. R. Dorfman, "Simple maps with fractal diffusion coefficients", Phys. Rev. Lett. **74**, 387–390 (1995).

[14] R. Klages and J. R. Dorfman, "Dynamical crossover in deterministic diffusion", Phys. Rev. E **55**, R1247–R1250 (1997).

[15] I. Percival and F. Vivaldi, "A linear code for the sawtooth and cat maps", Physica D **27**, 373–386 (1987).

[16] R. Strepparava, Laurea thesis, MA thesis (Universitá degli Studi di Milano, 1995).

[17] H.-C. Tseng, H.-J. Chen, P.-C. Li, W.-Y. Lai, C.-H. Chou, and H.-W. Che, "Some exact results for the diffusion coefficients of maps with pruning cycles", Phys. Lett. A **195**, 74–80 (1994).

Exercises

A24.1. **Recursion relations.** Verify that the following recursion relations are satisfied

$$u_{k+2} = \chi u_{k+1} - u_k$$

where $u_k = A_k, B_k, C_k, D_k$.

A24.2. **Arnol'd cat map.** Show that for $\chi = 3$, $A_k = F_{2k+1}$, $B_k = L_{2k+1}$, $C_k = L_{2k}$ and $D_k = 5F_{2k}$, where F_n and L_n are the Fibonacci and Lucas numbers..

A24.3. **Pruning rules for substrings of length 2.** Take $K = 8$ and draw the region determined by (A24.4).

A24.4. **Diagonalization of A.** Show that A can be diagonalized by considering the auxiliary matrix U

$$U \stackrel{\text{def}}{=} \begin{pmatrix} 1 & 1 & \cdots & 1 & 1 \\ \epsilon_0 & \epsilon_1 & \cdots & \epsilon_{T-2} & \epsilon_{T-1} \\ \vdots & \vdots & \ddots & \vdots & \vdots \\ \epsilon_0^{T-2} & \epsilon_1^{T-2} & \cdots & \epsilon_{T-2}^{T-2} & \epsilon_{T-1}^{T-2} \\ \epsilon_0^{T-1} & \epsilon_1^{T-1} & \cdots & \epsilon_{T-2}^{T-1} & \epsilon_{T-1}^{T-1} \end{pmatrix} .$$

In fact $U^{-1}AU$ is a diagonal matrix (the diagonal elements coinciding with $f(\epsilon_j)$).

A24.5. **Periodic points of cat maps.** Verify that (A24.15) is exactly the number of T–periodic points of the map when K is an integer.

A24.6. **Probability distribution.** Higher order moments can be computed easily for integer K (or generic K within the quasilinear approximation), by generalizations of (A24.17): show that the results prove that, given a period T, the distribution of periodic orbits with respect to their jumping number is asymptotically Gaussian, with parameter $D^{(q.l.)}$.

A24.7. **Deterministic diffusion, zig-zag map.**

To illustrate the main idea of chapter 24, tracking of a globally diffusing orbit by the associated confined orbit restricted to the fundamental cell, we consider a class of simple 1-dimensional dynamical systems, chains of piecewise linear maps, where all transport coefficients can be evaluated analytically. The translational symmetry (24.21) relates the unbounded dynamics on the real line to the dynamics restricted to a "fundamental cell" - in the present example the unit interval curled up into a circle. An example of such map is the sawtooth map

$$\hat{f}(x) = \begin{cases} \Lambda x & x \in [0, 1/4 + 1/4\Lambda] \\ -\Lambda x + (\Lambda + 1)/2 & x \in [1/4 + 1/4\Lambda, 3/4 - 1/4\Lambda] \\ \Lambda x + (1 - \Lambda) & x \in [3/4 - 1/4\Lambda, 1] \end{cases} . \tag{A24.19}$$

The corresponding circle map $f(x)$ is obtained by modulo the integer part. The elementary cell map $f(x)$ is sketched in figure **??**. The map has the symmetry property

$$\hat{f}(\hat{x}) = -\hat{f}(-\hat{x}) , \tag{A24.20}$$

so that the dynamics has no drift, and all odd derivatives of the generating function (24.3) with respect to β evaluated at $\beta = 0$ vanish.

The cycle weights are given by

$$t_p = z^{n_p} \frac{e^{\beta \hat{n}_p}}{|\Lambda_p|} . \tag{A24.21}$$

The diffusion constant formula for 1-dimensional maps is

$$D = \frac{1}{2} \frac{\langle \hat{n}^2 \rangle_\zeta}{\langle n \rangle_\zeta} \tag{A24.22}$$

where the "mean cycle time" is given by

$$\langle n \rangle_\zeta = z \frac{\partial}{\partial z} \frac{1}{\zeta(0, z)} \Big|_{z=1} = - {\sum}' (-1)^k \frac{n_{p_1} + \cdots + n_{p_k}}{|\Lambda_{p_1} \cdots \Lambda_{p_k}|} , \tag{A24.23}$$

the mean cycle displacement squared by

$$\langle \hat{n}^2 \rangle_\zeta = \frac{\partial^2}{\partial \beta^2} \frac{1}{\zeta(\beta, 1)} \Big|_{\beta=0} = - {\sum}' (-1)^k \frac{(\hat{n}_{p_1} + \cdots + \hat{n}_{p_k})^2}{|\Lambda_{p_1} \cdots \Lambda_{p_k}|} , \tag{A24.24}$$

and the sum is over all distinct non-repeating combinations of prime cycles. Most of results expected in this projects require no more than pencil and paper computations.

Implementing the symmetry factorization (24.18) is convenient, but not essential for this project, so if you find example 25.9 too long a read, skip the symmetrization.

A24.8. **The full shift sawtooth map.** Take the map (A24.19) and extend it to the real line. As in example of figure 24.3, denote by a the critical value of the map (the maximum height in the unit cell)

$$a = \hat{f}(\frac{1}{4} + \frac{1}{4\Lambda}) = \frac{\Lambda + 1}{4} . \tag{A24.25}$$

Describe the symbolic dynamics that you obtain when a is an integer, and derive the formula for the diffusion constant:

$$D = \frac{(\Lambda^2-1)(\Lambda-3)}{96\Lambda} \qquad \text{for } \Lambda = 4a-1,\ a\in\mathbb{Z}. \tag{A24.26}$$

If you are going strong, derive also the fromula for the half-integer $a = (2k+1)/2$, $\Lambda = 4a+1$ case and email it to DasBuch@nbi.dk. You will need to partition $\mathcal{M}_2$ into the left and right half, $\mathcal{M}_2 = \mathcal{M}_8 \cup \mathcal{M}_9$, as in the derivation of (24.28). See exercise 24.1.

A24.9. **Sawtooth map subshifts of finite type.** We now work out an example when the partition is Markov, although the slope is not an integer number. The key step is that of having a partition where intervals are mapped *onto* unions of intervals. Consider for example the case in which $\Lambda = 4a-1$, where $1 \le a \le 2$. A first partition is constructed from seven intervals, which we label $\{\mathcal{M}_1, \mathcal{M}_4, \mathcal{M}_5, \mathcal{M}_2, \mathcal{M}_6, \mathcal{M}_7, \mathcal{M}_3\}$, with the alphabet ordered as the intervals are laid out along the unit interval. In general the critical value a will not correspond to an interval border, but now we choose a such that the critical point is mapped onto the right border of $\mathcal{M}_1$, as in figure **??** (a). The critical value of $f()$ is $f(\frac{\Lambda+1}{4\Lambda}) = a-1 = (\Lambda-3)/4$. Equating this with the right border of $\mathcal{M}_1$, $x = 1/\Lambda$, we obtain a quadratic equation with the expanding solution $\Lambda = 4$. We have that $f(\mathcal{M}_4) = f(\mathcal{M}_5) = \mathcal{M}_1$, so the transition matrix (17.1) is given by

$$\phi' = T\phi = \begin{bmatrix} 1&1&1&1&0&0&1\\ 1&0&0&1&0&0&1\\ 1&0&0&1&0&0&1\\ 1&0&0&1&0&0&1\\ 1&0&0&1&0&0&1\\ 1&0&0&1&0&0&1\\ 1&0&0&1&1&1&1 \end{bmatrix} \begin{bmatrix} \phi_1\\ \phi_4\\ \phi_5\\ \phi_2\\ \phi_6\\ \phi_7\\ \phi_3 \end{bmatrix} \tag{A24.27}$$

and the dynamics is unrestricted in the alphabet

$$\{1,\ \underline{41},\ \underline{51},\ 2,\ \underline{63},\ \underline{73},\ 3,\}\,.$$

One could diagonalize (A24.27) on the computer, but, as we saw in chapter 17, the transition graph figure **??** (b) corresponding to figure **??** (a) offers more insight into the dynamics. The dynamical zeta function

$$\begin{aligned} 1/\zeta &= 1-(t_1+t_2+t_3)-2(t_{14}+t_{37}) \\ 1/\zeta &= 1-3\frac{z}{\Lambda}-4\cosh\beta\frac{z^2}{\Lambda^2}\,. \end{aligned} \tag{A24.28}$$

follows from the loop expansion (18.13) of sect. 18.3. The material flow conservation sect. 23.4 and the symmetry factorization (24.18) yield

$$0 = \frac{1}{\zeta(0,1)} = \left(1+\frac{1}{\Lambda}\right)\left(1-\frac{4}{\Lambda}\right)$$

which indeed is satisfied by the given value of Λ. Conversely, we can use the desired Markov partition topology to write down the corresponding dynamical zeta function, and use the $1/\zeta(0,1) = 0$ condition to fix Λ. For more complicated transition matrices the factorization (24.18) is very helpful in reducing the order of the polynomial condition that fixes Λ.

The diffusion constant follows from (24.19) and (A24.22)

$$\langle n\rangle_\zeta = -\left(1+\frac{1}{\Lambda}\right)\left(-\frac{4}{\Lambda}\right), \quad \langle \hat{n}^2\rangle_\zeta = \frac{4}{\Lambda^2}$$

$$D = \frac{1}{2}\,\frac{1}{\Lambda+1} = \frac{1}{10}$$

Think up other non-integer values of the parameter for which the symbolic dynamics is given in terms of Markov partitions: in particular consider the cases illustrated in figure **??** and determine for what value of the parameter a each of them is realized. Work out the transition graph, symmetrization factorization and the diffusion constant, and check the material flow conservation for each case. Derive the diffusion constants listed in table **??**. It is not clear why the final answers tend to be so simple. Numerically, the case of figure **??** (c) appears to yield the maximal diffusion constant. Does it? Is there an argument that it should be so?

The seven cases considered here (see table **??**, figure **??** and (A24.26)) are the 7 simplest complete Markov partitions, the criterion being that the critical points map onto partition boundary points. This is, for example, what happens for unimodal tent map; if the critical point is preperiodic to an unstable cycle, the grammar is complete. The simplest example is the case in which the tent map critical point is preperiodic to a unimodal map 3-cycle, in which case the grammar is of golden mean type, with _00_ substring prohibited (see figure 17.6). In case at hand, the "critical" point is the junction of branches 4 and 5 (symmetry automatically takes care of the other critical point, at the junction of branches 6 and 7), and for the cases considered the critical point maps into the endpoint of each of the seven branches.

One can fill out parameter a axis arbitrarily densely with such points - each of the 7 primary intervals can be subdivided into 7 intervals obtained by 2-nd iterate of the map, and for the critical point mapping into any of those in 2 steps the grammar (and the corresponding cycle expansion) is finite, and so on.

A24.10. **Sawtooth map diffusion coefficient, numerically.** *(optional:)*
Attempt a numerical evaluation of

$$D = \frac{1}{2}\lim_{n\to\infty}\frac{1}{n}\langle \hat{x}_n^2\rangle\,. \tag{A24.29}$$

Study the convergence by comparing your numerical results to the exact answers derived above. Is it better to use few initial $\hat{x}$ and average for long times, or to use many initial $\hat{x}$ for shorter times? Or should one fit the distribution of $\hat{x}^2$ with a Gaussian and get the D this way? Try to plot dependence of D on Λ; perhaps blow up a small region to show that the dependance of D on the parameter Λ is fractal. Compare with figure 24.5 and figures in refs. [6, 12–14, 17].

A24.11. **Sawtooth D is a nonuniform function of the parameters.** *(optional:)*
The dependence of D on the map parameter Λ is rather unexpected - even though for larger Λ more points are mapped outside the unit cell in one iteration, the diffusion constant does not necessarily grow. An interpretation of this lack of monotonicity would be interesting.

You can also try applying periodic orbit theory to the sawtooth map (A24.19) for a random "generic" value of the parameter Λ, for example $\Lambda = 6$. The idea is to bracket this value of Λ by the nearby ones, for which higher and higher iterates of the critical value $a = (\Lambda+1)/4$ fall onto the partition boundaries, compute the exact diffusion constant for each such approximate Markov partition, and study their convergence toward the value of D for $\Lambda = 6$. Judging how difficult such problem is already for a tent map (see sect. 18.5 and appendix **??**), this is too ambitious for a week-long exam.

A24.12. **Deterministic diffusion, sawtooth map.**
To illustrate the main idea of chapter 24, tracking of a globally diffusing orbit by the associated confined orbit restricted to the fundamental cell, we consider in more detail the class of simple 1-dimensional dynamical systems, chains of piecewise linear maps (24.20). The translational symmetry (24.21) relates the unbounded dynamics on the real line to the dynamics restricted to a "fundamental cell" - in the present example the unit interval curled up into a circle. The corresponding circle map $f(x)$ is obtained by modulo the integer part. The elementary cell map $f(x)$ is sketched in figure 24.3. The map has the symmetry property

$$\hat{f}(\hat{x}) = -\hat{f}(-\hat{x}), \tag{A24.30}$$

so that the dynamics has no drift, and all odd derivatives of the generating function (24.3) with respect to β evaluated at $\beta = 0$ vanish.

The cycle weights are given by

$$t_p = z^{n_p} \frac{e^{\beta \hat{n}_p}}{|\Lambda_p|}. \tag{A24.31}$$

The diffusion constant formula for 1-dimensional maps is

$$D = \frac{1}{2} \frac{\langle \hat{n}^2 \rangle_\zeta}{\langle n \rangle_\zeta} \tag{A24.32}$$

where the "mean cycle time" is given by

$$\langle n \rangle_\zeta = z \frac{\partial}{\partial z} \frac{1}{\zeta(0,z)}\bigg|_{z=1} = -\sum{}' (-1)^k \frac{n_{p_1} + \cdots + n_{p_k}}{|\Lambda_{p_1} \cdots \Lambda_{p_k}|}, \tag{A24.33}$$

the mean cycle displacement squared by

$$\langle \hat{n}^2 \rangle_\zeta = \frac{\partial^2}{\partial \beta^2} \frac{1}{\zeta(\beta,1)}\bigg|_{\beta=0} = -\sum{}' (-1)^k \frac{(\hat{n}_{p_1} + \cdots + \hat{n}_{p_k})^2}{|\Lambda_{p_1} \cdots \Lambda_{p_k}|}, \tag{A24.34}$$

and the sum is over all distinct non-repeating combinations of prime cycles. Most of results expected in this projects require no more than pencil and paper computations.